FLUID INJECTION THROUGH OUT-OF-PLANE MICRONEEDLES

Boris Stoeber (1), and Dorian Liepmann (2)

(1) Berkeley Sensor and Actuator Center – University of California at Berkeley – 497 Cory Hall – Berkeley, California, 94704 U.S.A. - Tel +1 (510) 642 4876, Fax +1 (510) 643 6637, Email boris@me.berkeley.edu
(2) Berkeley Sensor and Actuator Center – University of California at Berkeley – 497 Cory Hall – Berkeley, California, 94704 U.S.A. - Tel +1 (510) 642 9360, Fax +1 (510) 643 6637, Email liepmann@me.berkeley.edu

***Abstract* – In order to make frequent injections of insulin and other therapeutic agents more efficient, a new painless way to inject drug subcutaneously is investigated. Injecting such agents just under the stratum corneum is a painless and very effective way of drug delivery, since the nerve endings occur deeper under the skin, and the presence of a large number of capillaries help to absorb the drugs efficiently into the vascular system. The critical component for the successful development of this methodology is an array of robust, sharp, hollow microneedles. Arrays of needles that fulfill these requirements have been fabricated using a new fabrication process based on a combination of isotropic and anisotropic etching. Prototypes of these single crystal needles have been successfully tested by injection of fluid into chicken thighs. The flow characteristics of these needles have been modeled using the modified Bernoulli equation. This one-dimensional model has been validated through experimental results.**

I. INTRODUCTION

A. Need for Microneedles

Injection of lyophilized drugs just under the stratum corneum, which is the upper part of the skin, could present an extremely effective means for drug delivery. Since the nerve endings occur at a depth of about 100μm, delivery at this location will be painless. In addition, because of the presence of a large number of capillaries the drug will be effectively absorbed into the body. Perhaps more importantly, a delivery system for lyophilized drugs would provide the basis for the development portable systems that would have long shelf-life and be immune to temperature extremes. Furthermore, such a system would be ideal for drugs that are not effective when taken orally either because of poor absorbtion or side effects such as liver damage. Because of the potential simplicity and lack of pain, this approach could also make parenteral delivery much more palatable to patients. To achieve these goals requires a device that can deliver a controlled amount of drug in a distributed area at the correct depth below the skin. The critical component for the successful development of this methodology is an array of robust, sharp, hollow microneedles. Although a system could be developed which delivers a dry drug, the current work assumes that the lyophilized drug will be suspended in a non-aqueous, viscous fluid to prevent the drug from falling out of the device and to aid in complete delivery through the needle-array.

B. Requirements

A successful system will require sharp needles to easily penetrate the skin and a length of 100 μm in order to deliver drugs at the correct location. In addition, because the needles will typically experience lateral forces during injection that will induce bending moments onto their shafts, the needles have to be robust and be able to withstand these forces without breaking. Because any injection system will have to be disposable, the manufacturing cost will have to be low so the fabrication yield will have to be very high. Finally, the flow resistance for injection through these needles should be in a range where the necessary forces involved do not risk breaking the device.

C. Existing Microneedles

Needles fabricated through a combination of surface- and bulk-micromachining techniques where a silicon nitride shell is built on top of a silicon substrate [1] can only be aligned in the plane. Large two-dimensional arrays are not feasible using this fabrication technique.

Processes have been reported [2] that allow fabrication of two-dimensional arrays of polysilicon and metal needles. However the fabricated hollow metal needles have very thin walls that may not withstand the typical mechanical stresses associated with medical applications. The silicon needles are fabricated using a process [3] that gives irregular needles with a high surface roughness.

II. DESIGN OF OUT-OF-PLANE MICRONEEDLES

In order to satisfy the strength requirements mentioned above and for an easy penetration of the skin, a needle with a wide base and a pointed tip was designed. For easy handling and distributed delivery, the micro-needles are fabricated in large two-dimensional arrays perpendicular to the surface of the base material (Fig.1).

This research has been funded by the Becton Dickinson Technology Center under the management of Dr. Noel Harvey.

The outer shape of a needle is generated through isotropic underetching of a circular mask (Fig.1a). The resulting structure has a wide base and a slim shaft. The inner channel of the needle is obtained through an anisotropic etch (Fig.1b). These two surfaces generated through etching are symmetric with respect to their corresponding centerlines. If these centerlines are identical, the resulting needle is symmetric (Fig.1c). However, if both center-lines are parallel but dislocated by some distance δ, these two surfaces will generate a needle with a pointed tip on one side, as shown in Fig.1d.

Once the isotropic etch has been performed far enough that a pointed tip can be generated, the outline of the needle barely changes as the etch continues. Therefore, this process is insensitive to local etch rate variations.

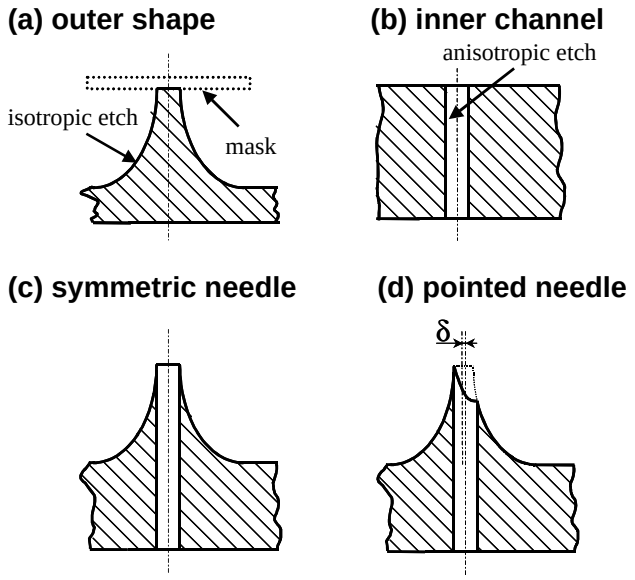

Fig. 1. Design of a needle. a) Isotropically etched outer shape, b) anisotropically etched channel, c) symmetric needle obtained through overlaying the center lines of (a) and (b), d) pointed needle, where the center lines of the outer shape (a) and the inner channel (b) are dislocated by the distance δ.

III. FABRICATION PROCESS

The fabrication process for out-of-plane microneedles is illustrated in Fig.2. It is a two-mask process that involves standard photolithography and a combination of isotropic and anisotropic etching.

1. A 550μm thick double-sided polished single crystal silicon wafer is coated with 6mm of silicon dioxide as a mask material using a LPCVD process.

2. The oxide layer on the backside of the wafer is then patterned with 40μm diameter holes using photolithography followed by a CF_4 – CHF_3 – He plasma etch.

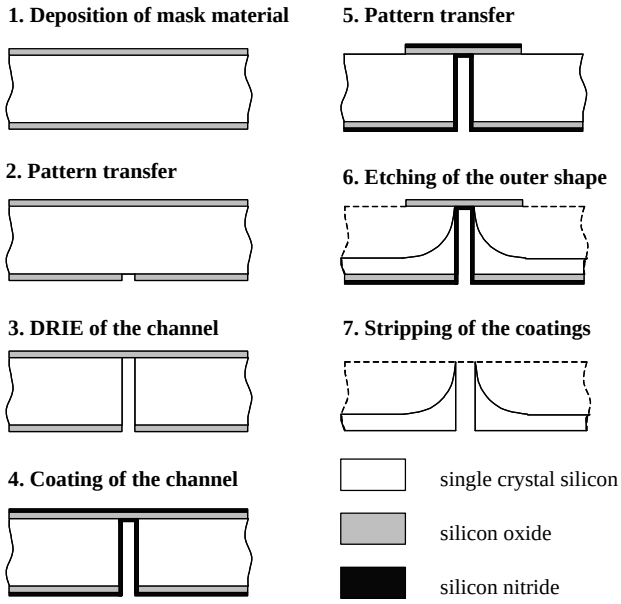

Fig. 2. Process flow for the fabrication of out-of-plane microneedles

3. The channels of the needles are defined through deep reactive ion etching (DRIE) all the way through the wafer stopping on the upper oxide layer.

4. Silicon nitride is deposited at a thickness of 0.4μm using LPCVD in order to protect the channels during a following etch step.

5. Disks with diameters of 425μm are patterned into the front side using the same techniques as in step 2. The front side pattern is aligned to the beachside features using a Karl Suss mask aligner.

6. These circular masks are isotropically underetched using an SF_6 plasma to a depth of 150μm first, which is a fast etch that generates a high surface roughness. An isotropic wet chemical etch for another 50μm completes the etch of the outer shape of the needle while smoothening the surface of the structure. As the isotropically etched surface intersects with the channels, the silicon nitride will act as an etch stop and protect the sidewalls of the channels.

7. Finally, the layers of silicon oxide and silicon nitride are removed in concentrated HF for 12 hours.

IV. FABRICATED DEVICES

Using the process presented above, arrays of up to 8 needles per die have been fabricated with a channel diameter of 40μm and a height of 200μm. Fig.3 shows an array of symmetric needles. The needles represented in Fig.4 have pointed tips with radii of curvature of about 10mm. A smaller radius of curvature would make it easier for the needles to break the skin, and can be obtained by optimizing the process parameters.

Both symmetric and asymmetric structures are highly uniform, and a yield of 100% across a wafer has been achieved.

The distance between the needles shown in Fig.3 and 4 is 750μm. Needle density could be increased up to the limit

given by the diameter of the circles (425μm) on the front side mask. This would result in the maximum density $n = N/A = 640/cm^2$, number of needles, N, per surface area A. Since the flow resistance of a device decreases with the number of needles, a high number would reduce the pressure drop. However, too high a density could reduce the efficiency of needle penetration through the skin.

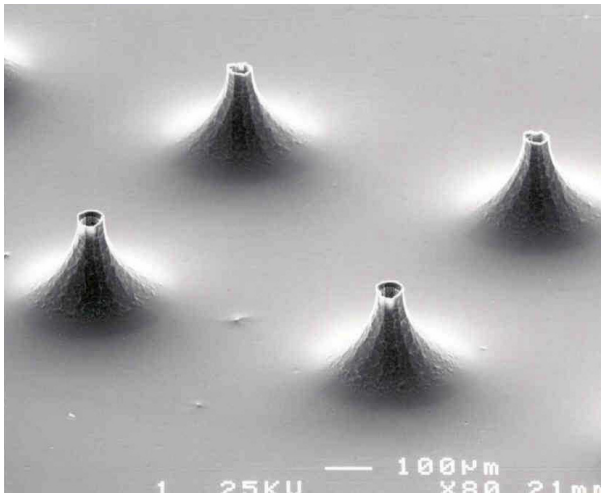

Fig. 3. Array of symmetric needles; channel diameter d=40μm, height h=200μm, distance between needles: 750μm.

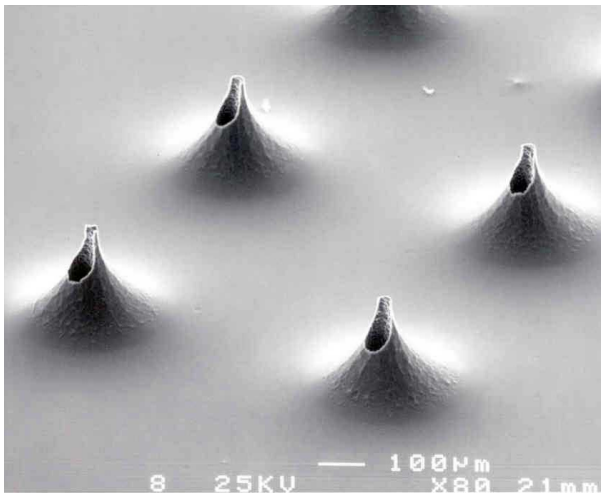

Fig. 4. Array of pointed needles, channel diameter d=40μm, height h=200μm, distance between needles: 750μm, dislocation δ=20μm.

V. NEEDLE PERFORMANCES

A. *Injection of Liquid through Microneedles*

In order to investigate the ability of the microneedles to inject material into tissue, a single needle with a sharp tip was used to deliver a fluorescent dye, Lucifer Yellow, into a chicken thigh. The result, shown in Fig.5 and Fig.6 indicates that the fluid was successfully delivered more than 100μm under the skin. The pictures were taken through confocal microscopy.

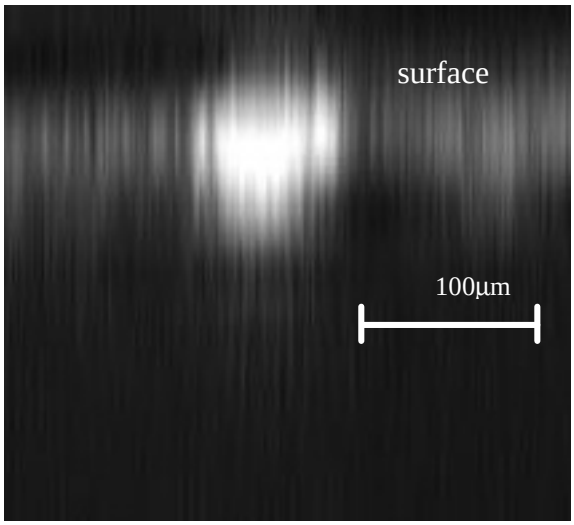

Fig. 5. Cross section of chicken tissue. Fluorescent Lucifer Yellow has been injected and detected using confocal microscopy.

A critical design requirement for a micro-needle is that it does not break during an injection. Fig.6 shows a needle

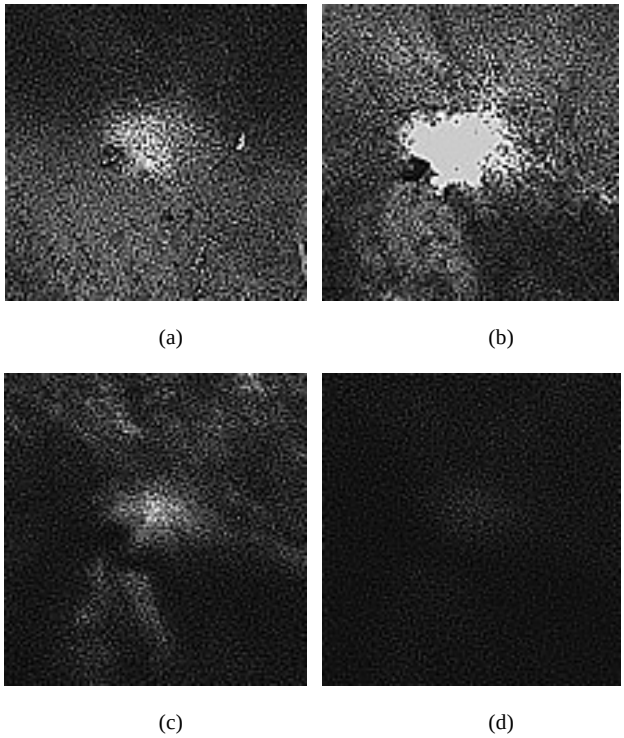

Fig. 6. Planes parallel to the surface of the chicken tissue. The pictures are taken using confocal microscopy where the focal plane is in the following depths below the chicken skin: a) 0μm, b) 25μm, b) 75μm,

before and after it was penetrated into a chicken breast ten times. As demonstrated in the figure, there is no visible damage which indicates that this design will be strong

enough to withstand the forces associated with a typical application.

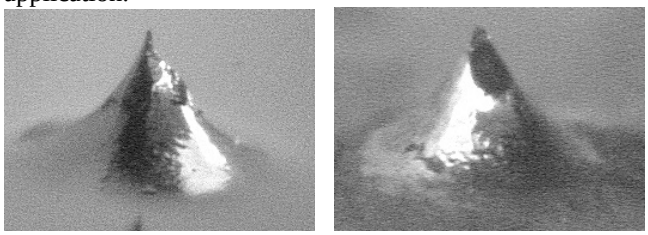

Fig. 6. Needle before (left) and after (right) ten injections into chicken. The needle has not been damaged.

B. Flow Characteristics

1) Theoretical Approach : The pressure drop Δp as a function of flow rate q for an individual symmetric needle as shown in Fig.7 has been modeled using the modified Bernoulli equation [4],

$$p_1 - p_2 + r\,\frac{v_1^{\,2} - v_2^{\,2}}{2} + r\,g(z_1 - z_2) = r\,f\,\frac{L}{d}\,\frac{v^2}{2} + \sum r\,K\,\frac{v^2}{2}, \qquad (1)$$

which is generally used to describe fluid flow through macroscopic piping systems. The subscripts 1 or 2 refer to the entrance or exit of the needle respectively. It can be shown that the influence of gravity can be neglected compared to the right hand side of (1). For a channel with a constant cross sectional area as in the case of the needle considered, (1) can further be reduced to

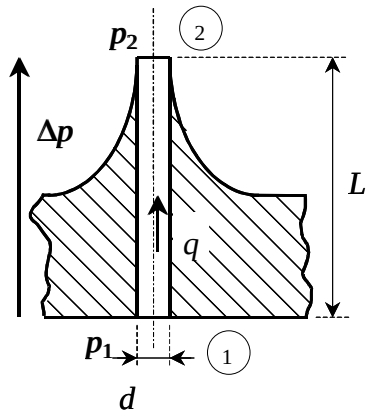

Fig. 7. Flow through a symmetric needle.

$$\Delta p = m\,\frac{128}{p}\,\frac{q\,L}{d^4} + r\,\frac{8}{p^2}\,\frac{q^2}{d^4}(K_1 + K_2), \qquad (2)$$

where the friction factor $f = 64/\mathrm{Re}$ for laminar flow has been used. K_1 and K_2 describe the minor losses at the entrance and at the exit of the needle respectively. Standard macroscopic values for a square edged inlet ($K_1 = 0.5$) and for an exit ($K_2 = 1.0$) are chosen [4] to describe the minor losses of systems. The first term on the right hand side of (2) describes the pressure drop induced by the viscous shear force of Poiseuille flow inside a circular tube [5], while the second term corresponds to inertia effects at the entrance and exit.

2) Experimental Results : The pressure drop vs. flow rate for arrays of two and eight needles has been measured using water. Figure 8 compares the experimental results with the theoretical values. For the array of 8 needles, the error is smaller than 2%, while the measurement accuracy is estimated at 3%. For the array of 8 needles, 30 measurements per data point have been used as opposed to only 20 readings for the array of 2 needles. Assuming that the larger number of needles have an averaging effect on the result, the measurement for the array of 8 needles involves a six more sets of experimental values. This explains error reduction relative to the 2 needle array

The maximum Reynolds number for this experiment is $\mathrm{Re} = 330$ at a flow rate of $q = 5000\mu$l/min through 8 needles. The assumption of laminar flow made previously is therefore justified.

C. Robustness of the Device during Injection

An array of needles could be fabricated that has half the maximum density n of needles on a disc with a diameter of 1cm, that means $N = 250$. A typical application, where 100µl of aqueous fluid is injected through these needles within 2s, would require a pressure $\Delta p = 1.78$kPa according to (2). In order to get a rough estimate of the stress generated in the ground plate, it will be modeled as clamped round plates between three neighboring needles that will be supporting the structure from the skin during the injection. The maximum stress [6]

$$s = 0.75\,\Delta p\,R^2/t^2 \qquad (3)$$

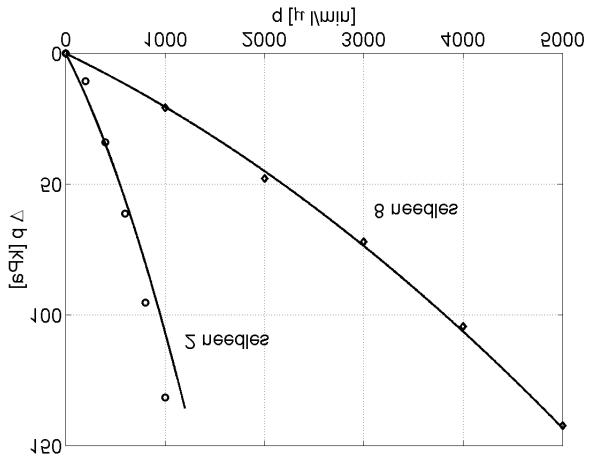

Fig. 8. Pressure drop Δp as a function of flow rate q for arrays of 2 and 8 needles; theory [-], measurements [o]; error of the measurements of the array of 8 needles: 2%, accuracy: 3%.

in a circular plate with constrained edges, an effective radius R = 0.32mm and a thickness t = 0.35mm

$$s = 1.12\,\text{kPa}$$

is $3.4 \cdot 10^6$ times smaller than the yield strength σ_y = 3.8GPa of silicon [7]. Even if the flow assumptions and pressure drop into the tissue increased the pressure drop by two orders of magnitude, the maximum stress would still be 34000 times higher than σ_y. The device should therefore be sufficiently strong for typical biomedical applications.

VI. CONCLUSION

A new fabrication process has been presented for production of arrays of micro needles. These needle arrays are an important step in the development of novel drug delivery system where therapeutic agents are injected just under the upper layer of the skin. These needles have been successfully tested on chicken thighs. A model that describes their flow characteristics has been developed and experimentally validated. It has been shown that the device is robust enough to withstand the stresses generated during a standard application for drug delivery.

Further work is needed to predict the performance of a complete drug delivery system based on these arrays of needles. It will be necessary to characterize the flow impedance by the involved tissue. Further, the dynamic behavior of such a system should be investigated, since it can be assumed, that transient effects play an important role in the practical application for drug delivery.

ACKNOWLEDGMENTS

The authors would like to thank the staff of the Berkeley Microfabrication Facility for their advice and support, and Ron Wilson for taking the SEM pictures used in this paper. Further thanks are addressed to Dr. Steven E. Ruzin for taking the pictures with the confocal microscope, as well as to Martin Decaris for his assistance in taking the measurements presented.

NOMENCLATURE

Symbol	Meaning
A	surface area
d	channel diameter
f	friction factor
g	gravitational acceleration
h	needle height
K	coefficient for a minor loss
L	channel length
n	density of needles per unit area
N	number of needles
p	pressure
q	volumetric flow rate
R	radius
Re	Reynolds number
t	thickness
v	flow velocity
z	height
δ	dislocation
Δp	pressure drop
μ	viscosity
ρ	density
σ	stress
σ_y	yield strength
$(\,)_1$	value at the channel entrance
$(\,)_2$	value at the channel exit

REFERENCES

[1] Lin, L., and Pisano, A.P., "Silicon-processed microneedles," Trans. IEEE J. of Microelectromechanical Systems, vol.8, no.1, pp.78-84, 1999.

[2] McAllister, D.V., Cros, F., Davis, S.P., Matta, L.M., Prausnitz, M.R., and Allen, M.G., "Three-dimensional hollow microneedle and microtube arrays," Transducers '99, pp.1098-1101, 1999.

[3] Henry, S., McAllister, D.V., Allen, M.G., and Prausnitz, M.R., "Microfabricated microneedles: A novel approach to transdermal drug delivery", Journal of Pharmaceutical Sciences, vol.87, no.8, pp.922-925, 1998.

[4] Janna, W.S., "Design of Fluid Thermal Systems," PWS-Kent Publishing Company, Boston, 1993.

[5] Batchelor, G.K., "An Introduction to Fluid Dynamics", Cambridge University Press, Cambridge, 1967.

[6] Beitz, W., Küttner, K.-H., Dubbel – Handbook of Mechanical Engineering, Springer-Verlag, London, 1994.

[7] Gauthier, M.M., "Engineered Materials Handbook, Desk Edition", ASM International, Materials Park, OH, U.S.A., 1995.